YOLO and Morphing-based Method for 3D Individualised Bone Model Creation

1st Zuzanna Krawczyk
Electrical Engineering Department
Warsaw University of Technology
Warsaw, Poland
zuzanna.krawczyk@ee.pw.edu.pl

2nd Jacek Starzyński
Electrical Engineering Department
Warsaw University of Technology
Warsaw, Poland
jstar@ee.pw.edu.pl

***Abstract*—The paper presents an automated tool for individualised skeletal model creation and identification of specific bone structures from computed tomography (CT) images. Contrary to the classical segmentation methods, the presented one is aimed at exact recognition of the bone joints. It takes advantage of a reference skeletal model. The developed procedure relies on the neural network detection of the bounding boxes to select single bones from CT slices. In the subsequent steps the reference model elements are matched to the detections by means of affine transformation and next, by morphing algorithm. The method incorporates various image processing algorithms including swarm intelligence heuristic algorithm—Artificial Ant Colony (enriched with an original pheromone deposition function). Three-dimensional models of bones created by the procedure can be used in the task of automatic delineation of bone structures, positioning of the patient for radiotherapy or in planning of orthopaedic medical procedure. They can also serve as a visual help in diseases detection.**

***Index Terms*—Coherent Point Drift (CPD), deep learning, image segmentation, individualised model, morphing, You Only Look Once (YOLO)**

I. Introduction

Individualised models of bone structures find wide application in the medical field including virtual bone representation in Computer-Assisted Orthopaedic Surgeries [1], creation of individualised templates [2] or implants [3]. Another interesting application is human motion analysis and its influence on the development of disorders [4], [5]. Individualised models are also useful in automatic delineation of critical organs [6] in radiotherapy planning or in Dynamic Adaptive Radiotherapy which employs advanced imaging techniques and patient positioning methods in order to modify the treatment plan in the real-time [7].

The traditional way of creation of individualised bone models out of the computed tomography (CT) data is based on manual or semi-manual segmentation of skeletal structures. It is a time-consuming process and has to be performed by qualified personnel. Automation of this process is not a trivial task due to numerous reasons: the differences in structure between trabecular and cortical bone are observable differently in imaging data, which makes the choice of one arbitrary segmentation method difficult. In particular, the border between the bones within joints is often unclear or invisible (see Fig. 1). Moreover, the same type of the bone can have a different shape depending on the age, sex or health condition of the examined person. Imaging data can be collected with numerous equipment having different capabilities. Patient position during examination may also vary. Thus, the transition from a set of two-dimensional images to three-dimensional structure is usually not offered by the imaging system providers.

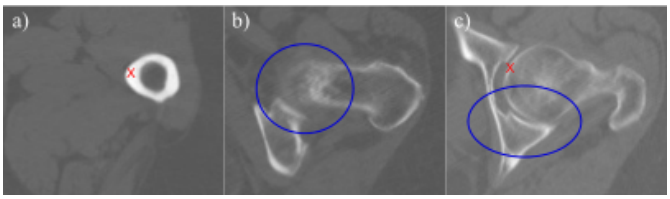

Figure 1. Examples of CT images representing cross-sections of the same femur bone taken on different heights. Points marked with red cross have the value of 1363 HU and 325 HU in images a) and c) respectively. The areas surrounded with blue ellipse in cross-sections b) and c) illustrate the region where femur head and pelvic bone are close to each other which makes them difficult to distinguish. Moreover in cross-sections b) and c) the boundaries of bone structure are unclear in contrast to cross-section a).

The paper introduces an automated method of creating individualised three-dimensional skeleton models out of CT data sets. The task is performed by extracting bones one by one and thus, for simplification, the method will be described here on the basis of the pelvis area with focus on the femur bone.

The presented approach makes use of the reference skeleton model (kept in form of the triangular surface mesh) which is transformed in a series of steps into the target individual model. In the first step the You Only Look Once (YOLO) neural network is employed to gain the knowledge about the correct shape of the bone structures and mutual position of the bones. It allows to extract the 3D image (in form of 2D pieces) of the processed bone from the CT data. Then a series of transformations of the reference model is used to fit it to the bone image extracted from CT series.

The paper is organised as follows: in the first chapter we review different earlier approaches to creation of individualised bones models; in the second chapter we present the details of our method and algorithms used; the third

978-1-7281-6926-2/20/$31.00 ©2020 IEEE

chapter presents the results obtained and discusses the choice of method parameters. The last chapter is focused on the conclusions and prospects for the further work.

II. Literature Review

Individualised bones models creation, out of medical data, is a non-trivial problem widely discussed in scientific papers. We can distinguish two approaches toward bones models creation. In the first approach, the model is created only using image processing methods, in the second one, the external knowledge database or reference model of the structures is employed.

The method proposed in [8], is an example of the first approach and presents automatic bone segmentation method based on operations of image filtering, wavelet analysis, histogram equalisation and region growing, but it is applied only to 2D series of data and does not include 3D model creation step. In [9] adaptive threshold algorithm is used in order to perform bone structure segmentation. In both papers, various bones are not distinguished. On the other hand, authors of [10] use pressure analogy to segment and distinguished two adjacent bones from each other. The method is a combination of various image processing algorithms, especially morphological operations. The method gives interesting results but in some cases, the created models are corrupted with defects in femoral head or parts of pelvis or veins are over-segmented and wrongly classified as a part of the model.

The methods falling in the second category often take use of a set of bones structures model called atlas. Such methods are more robust towards local artefacts than methods purely based on image processing. A good example of the automatic segmentation method based on adjustment of the atlas model to the bone structures visible on X-ray images is [11]. It is however constrained to 2D images. In [12] an atlas-based method aimed at pre-clinical planning in pelvic region is presented. It incorporates non-affine image transformation, but the results are still not satisfactory. The authors stress that separation of femur bone from the pelvis is a problem which needs further research.

Another widely used approach are Statistical Shape Models (SSM). Several papers describes their application to segmentation of femur and pelvic bones out of CT or MRI data [13]–[16]. SSMs are parametrised models created on the basis of a training set consisting of multiple shapes. They represent the normal shape variation of the training set. SSMs address the problem of wide variability of shapes of biological structures. Main drawback of the solutions based on SSMs is the cumbersome process of their creation. It consists of manual segmentation of training data set, creation of landmarks in the data and generation of the averaged model.

Recently convolutional neural networks (CNN) are more and more widely used in the field of digital imaging and visualisation. They also find application in medical data processing. In [17], [18] the usage of U-net network for segmentation and classification of bone structures to certain groups is shown. The analysis of various CNN architectures applied to segmentation of upper extremity of the femur bone is presented in [19]. The [20] shows the segmentation of 49 bones out of CT scans performed by another CNN network. All of the results are promising but in order to be effective the training of CNN networks performing segmentation task requires a large amount of medical data, which are not easily obtained.

III. Method

The method developed by the authors combines the atlas based-approach with the usage of CNN, what increases the level of automation. The reference skeletal model is a triangular surface mesh of a simplified male skeleton, which consists of 96 bones and of 123306 triangles in total. The bones within the skeleton are labelled. The whole skeleton is used to position the individualised model with respect to CT data, whereas individual bone meshes are being transformed to create the final model.

The algorithm consists of three main steps:

1) **Detection of the bone structures on the CT data series:** 2D bounding boxes are created around bone structures, on each CT slice on which femur bones are present. The dimensions of the bounding box correspond to the maximum dimensions of the structure they surround. The detection of the bounding boxes is performed by YOLO network.
2) **Affine transformation of the reference model mesh to fit it to CT based data:** The bounding cuboid surrounding the ordered series of bounding boxes of a given bone is created. Reference model of the femur is scaled to the dimensions of the cuboid and afterwards translated to the cuboid position.
3) **Non-affine transformation of the reference mesh to real bone structure characteristic:** In the last step the cross-sections of the previously prepositioned model mesh, positioned on the level of individual CT slices are created. Then, the cross-sections are scaled to dimensions of corresponding bounding boxes. The CT data are constrained to the size of the bounding boxes as well. After that, the edges of the bone structures are detected by the fusion of various edge detection and segmentation methods. In the following step the representational points, lying on the bone edges are chosen. The reference mesh is transformed by non-affine morphing algorithm to fit those points.

A. Detection of the bone structures in CT data

In the first step of the method, the detection of the bone structures on the series of CT data is performed. Femur and pelvis bones are marked with 2D bounding boxes. In order to automate this procedure, the YOLO (You Only Look Once) [21] neural network is used to detect the structures.

The training set consisted of 320 monochrome images, taken from two CT series of pelvis and its surrounding. One CT was registered for female and the second for a male patient. All of the images represent body sections in the transverse plane. Some of images represented full cross-section of patient

abdomen and some only a single bone structure. The contrast of images was diverse. The training set contained also negative samples without desired bone structures. 10% of the images were randomly chosen as the validation set. The network was trained for 1000 epochs. Sample results of detection are shown in the Fig. 2. The details of the network training and its parameters are presented in [22].

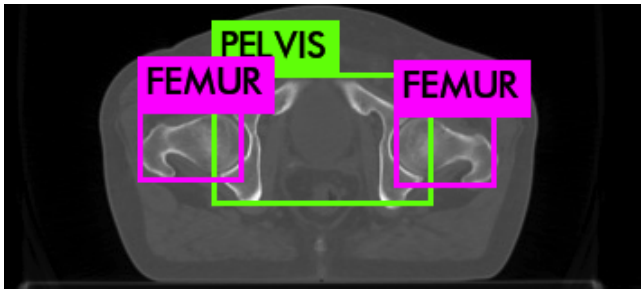

Figure 2. The sample detection of the femur and pelvis bone structures performed with YOLO. The pelvis is detected with 87.62% confidence and both femurs with over 90% confidence.

B. Affine transformation of the reference model

The bounding boxes detected by the YOLO network around the individual bone structures in the series of CT data are further used for the initial affine transformation of the reference model. For each previously defined and detected class of a bone structure, a 3-dimensional bounding contour is created. The bounding contour is a rectangular grid corresponding to the shape of the series of bounding boxes detected by the neural network for a given CT data series. Bounding contour is created on the basis of series of CT images and informations written in DICOM format such as: position of the CT slices, spacing between slices or image dimensions. In order to create bounding contour the following steps are performed:

1) The class of the bone for which the bounding contour is created is chosen.
2) The images from CT series are sorted along the longitudinal axis of the patient.
3) For each CT slice in series, if there is a corresponding bounding box (or bounding boxes of particular bone), a layer of mesh is created with length and width of bounding box and height equal to spacing between slices.

In the following step the bounding cuboid C_{TK} is created for the bounding contour of the pelvis bone (see Fig. 3). Analogues cuboid is created for the reference mesh of the pelvis bone C_{Ref}. The examples of both bounding contour and cuboid are presented in Fig 3. Individual bones of the reference model are scaled and translated so that position of cuboids C_{Ref} and C_{CT} is the same. Next, the cross-sections of transformed reference mesh models is created in the plane of each CT slice from the series. The dimensions of the cross-sections are scaled to match the dimensions of the appropriate bounding boxes. Each CT slice in data series is cut to the dimensions of the bounding contour as well.

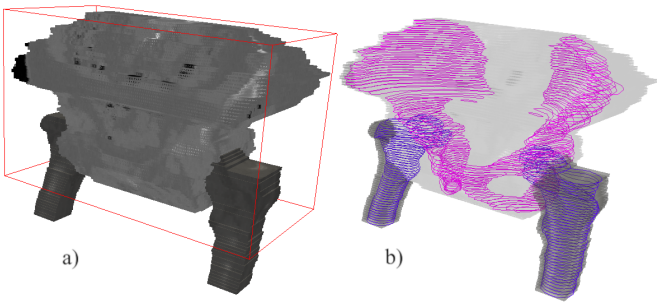

Figure 3. a) Bounding contours of pelvic bone and both femur bones with bounding cuboid C_{CT} of pelvis (red colour); b) Cross-sections of reference mesh model after scaling operation.

C. Non-affine transformation

In the final step the reference mesh is further adjusted by the morphing algorithm. In order to perform the transformation, the cloud of points P_C lying on the surface of the patient bone structure has to be created. The fusion of several methods is used for that purpose.

In the first stage three different edge detection operations are independently applied to the image I representing a bone structure:

- Canny edge detection algorithm,
- Laplacian of Gaussian (LoG) detection algorithm,
- modified Artificial Ant Colony (AAC) algorithm.

The above mentioned algorithms are based on different approaches each: Canny edge detection algorithm measures strength of the edge in the image by computing first-order derivative expression while LoG algorithm is looking for a zero-crossing in second-order derivative expression. The AAC algorithm is a heuristic swarm intelligence method, primarily used in the shortest path problem. The version used in the paper is adapted to image segmentation and edge detection as described in [23]. The number of iterations of AAC algorithm is set to 500 and the number of swarm agents (due to large number of the pixels representing the bone structure in the image) is set to 70% of the number of pixels in the image. The rest of the AAC parameters is set as described in [24].

The results of edge detection algorithms applied to the same image are slightly different which depends on the level of sensitivity of the algorithm to the noise present in the image, the type of smoothing filter used, the method of defining the edges, or other details of the method implementation. The LoG algorithm was chosen for the method because it creates thin, continuous and if possible closed edges. Rounding the corners in edges is the algorithm drawback. The Canny edge detection is one of most commonly used edge detection algorithms and it produces optimal results according to the conditions created by its authors [25]. The AAC algorithm separates two different bone structures more effective than Canny algorithm, but the created edges are thicker than in case of Canny or LoG algorithm. The application of three edge detection algorithms to the image I results in three binary images BA, BB and BC representing the same bone structure (see Fig. 4 and Fig. 5).

It is clear, that the images are different. Each of the edge detection algorithms has some advantages and drawbacks. To compensate those deficiencies the fusion of the results of three above-mentioned image processing algorithms is performed: this process consists of detecting points lying on the edges of the bone structure for each of the applied image processing algorithms, followed by the selection of points common for at least 2 of the 3 used algorithms. Additionally, the point detection is performed by two different methods applied to each binary image.

The first method of points detection uses a set of rays starting radially from the center of binary image towards the image boundary. The rays are arranged in equal angular distances with respect to each other, in the range from 0° to 360°. For each ray the method finds the white pixel with the furthest distance to the image center. The coordinates of the pixel are added to the set of points P_R potentially located on the surface of bone structure.

The second method of points detection uses horizontal and vertical segments connecting opposite borders of an image. The segments are arranged with the equal step w along the image border. For each segment the coordinates of first and last white pixel are added to the set of points P_L and considered as potentially located on the bone surface.

As a result of this step of the procedure 6 sets of points are created: three P_R sets are generated by the first point detection method and another three P_L sets are generated by second point detection method respectively.

In the following step the P_R sets are merged into one. Only the points detected by at least two of three binary images are promoted. The P_L sets are processed analogically, giving another set. Finally the two resulted sets are combined into the final one, by averaging points positions. Example of points detection performed by first method and final point set detected for CT slice is shown in the Fig. 4.

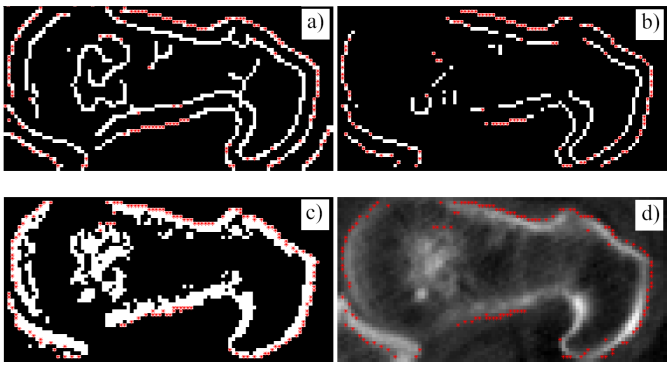

Figure 4. Example of result of edge detection methods with points selected by the first method marked with red colour: a) Canny edge detection b) *LoG* c) *AAC* algorithm d) input grey-scale image with final set of points.

The above procedure is performed for each image I from a series of CT slices cut to the dimensions of bounding contour. The points detected for all slices form 3-dimensional cloud of points P_C. The simplified scheme of the method is presented in the Fig. 5.

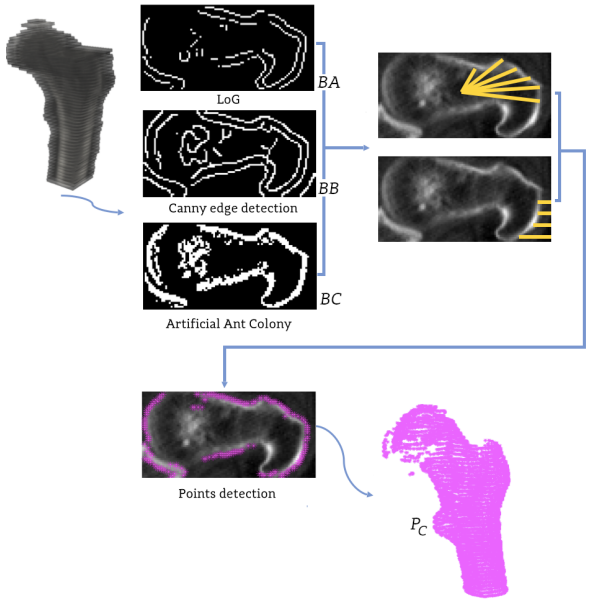

Figure 5. Creation of cloud of points P_C used to build the surface of the bone structure: the outline of the procedure.

The reference mesh, roughly prepositioned to the affine CT data, in general case, does not coincide with cloud of points P_C due to variety of positions of the patient during the medical examination, individual differences in the shape of the bone and simplified shape of the reference mesh. Hence, the need of non-affine adjustment of the model mesh to P_C point cloud. The number of P_C points is usually different than the number of vertices of the model mesh. The non-affine transformation has to find the approximation of the displacement of individual nodes of the model mesh to P_C. The problem is solved by the morphing algorithm called Coherent Point Drift (CPD).

Coherent Point Drift algorithm is a probabilistic, iterative point registration method described in [26]. In CPD algorithm the alignment of two point clouds is defined as a probability density estimation problem. The vertices of the reference mesh P_M are treated as Gaussian Mixture Model centroids and fit to the set of observations (which in described problem is the cloud of points P_C). The fit is done by maximisation of the likelihood function. The method imposes the coherent movement of the mesh vertices to preserve the topology of the set of points. It is done by Tikhonov regularization applied to the transformation field. The result of CPD transformation, represent the final bone model adjusted to the characteristic of individual patient. The visualisation of the morphing process is presented in the Fig. 6.

IV. Results

A. Test data

In order to validate the described approach the developed code was employed to creation of eight individualised models of femur bones. Four series of CT images of prostate cancer patients, representing the pelvic region were obtained due to courtesy of Maria Sklodowska-Curie National Research

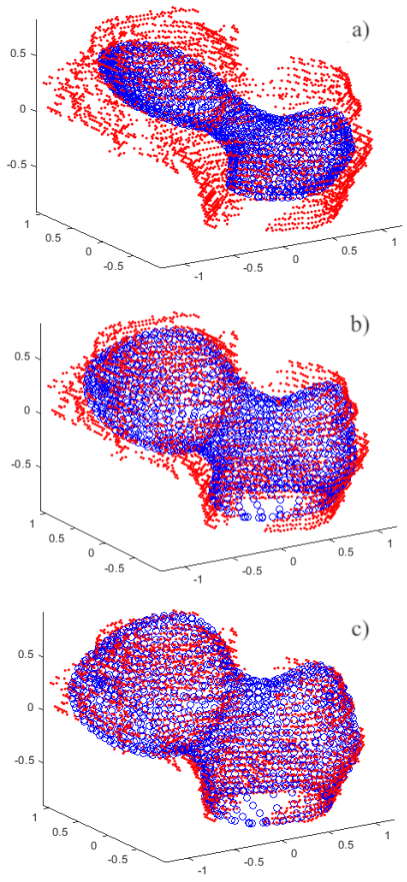

Figure 6. Subsequent stages of the morphing transformation (CPD algorithm) of femur bone a) 10th b) 15th c) 50th iteration; point cloud P_D – marked with red colour; vertices of the reference mesh – marked with blue circle.

Institute of Oncology. The detailed parameters of each series are presented in Table I. All of test cases were performed for Head First-Supine patient position. Two individualised models of femur bone, left and right, were created per each CT data set.

Table I
PARAMETERS OF TEST CT SERIES

Series No.	No. of CT slices	No. of pixels in slice	Voxel spacing
1	157	512x512	1.5625x15625x2.5
2	220	512x512	1.5625x15625x2.5
3	181	512x512	1.5625x15625x2.5
4	130	512x512	1.5625x15625x2.5

The eight exact expert models were created to compare them with meshes obtained by the automated morphing method. The CT data contained delineations of femurs upper extremities (most complex part of the bone by means of its shape), performed by an experienced professional. The delineation of the lower part of femur was created manually or semi-manually with the use of level-tracing method in 3D Slicer program. Further the two-dimensional delineations were connected into three-dimensional triangular mesh.

The expert model to which the created mesh is compared is burdened with errors—the resolution of the CT data does not allow to determine the exact boundary of the bone structure, and the identification it is the task of an expert. For some of the model cross-sections, it is unclear whether the contour created by the expert or detected automatically by the morphing algorithm more accurately represents the bone border. Therefore, the value of the measure of similarity between the expert mesh and the mesh created with the morphing method will never be equal to 100%.

B. Results of the method

The individualised models created by the method visually match the data, what can be seen in the Fig. 7, where femur meshes were imposed on simple segmentation of CT data (threshold equal to 100 HU). To perform quantative assessment

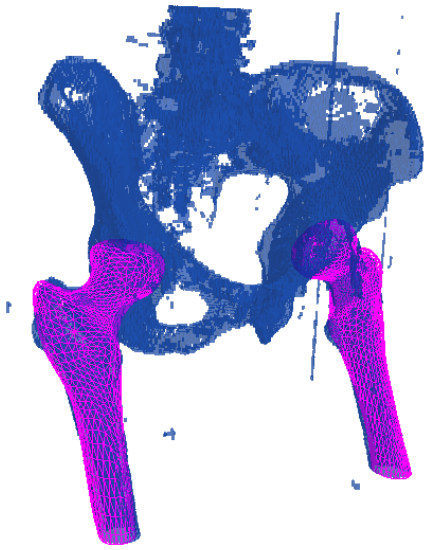

Figure 7. CT series No. 1: Individualised femur models (pink colour), created with the described method imposed on simple segmentation of CT data (blue colour), with 100 HU threshold.

of the fit, result meshes were compared with expert model by computing Jaccard index value:

$$J(V_e, V_m) = \frac{V_e \cap V_m}{V_e \cup V_m}, \tag{1}$$

where V_e is the volume of expert mesh and V_m the volume of mesh created with the use of described method. The Jaccard similarity measure was also evaluated for affine fit described in section III-B. The results of the similarity measure are presented in Table II.

The examples of the fit of the expert and individualised mesh can be seen in Fig. 8. Developed method creates femur mesh models with the accuracy within the range from 77.24% to 80.83%, which suggests good agreement of the model with the real data. The value of similarity measure is higher than in case of affine transformation. Moreover, due to use of the reference mesh in the transformation process the created model does not contain artefacts such as additional holes and islands, it is smooth and manifold.

Table II
SIMILARITY MEASURE BETWEEN EXPERT MESH AND TRANSFORMED REFERENCE MESH FOR LEFT (L) AND RIGHT (R) FEMUR BONE.

Series No.	Bone structure	Affine fit	Method fit
1	L	20.99%	80.83%
	R	27.54%	80.73%
2	L	14.60%	78.44%
	R	12.48%	77.24%
3	L	29.08%	77.53%
	R	23.75%	80.16%
4	L	21.01%	79.11%
	R	21.24%	78.66%

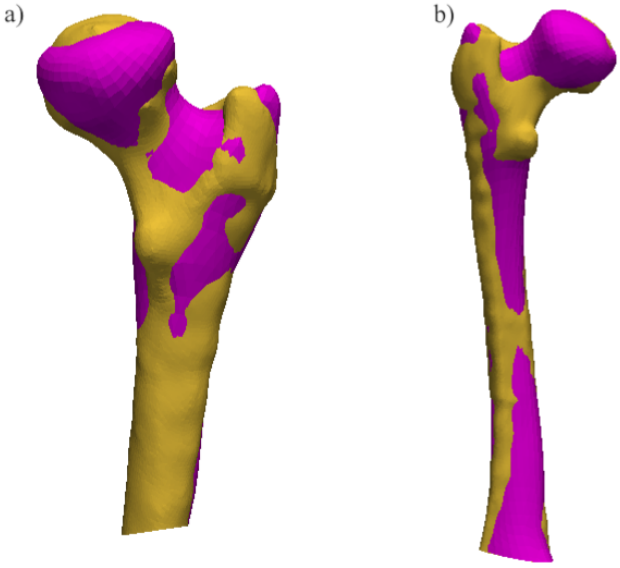

Figure 8. Expert mesh (yellow colour) and transformed individualised mesh (pink colour): a) left femur, CT series 1 b) right femur, CT series 2.

Further, the model created with the help of the morphing algorithm was compared with a second model created only with the combination of various image processing algorithms described in [28]. Both models are depicted in Fig. 9. The femoral head of the second model is under-segmented. Medullary cavity and part of the pelvis above the femoral head were also wrongly included in the model. The mesh model created with the use of morphing algorithm does not have those drawbacks.

In order to compare the method with another deep learning approach the U-net network was trained with similar amount of data as YOLO network. The results obtained with U-net were not satisfactory, due to limited number of training data, thus we do not publish them in the paper.

C. Adjustment of method parameters

The results of Canny and LoG detection algorithm are dependent on the values of their input parameters. In case of both algorithms, their values have an influence on the sensitivity of edge detection. Only edges for which gradient

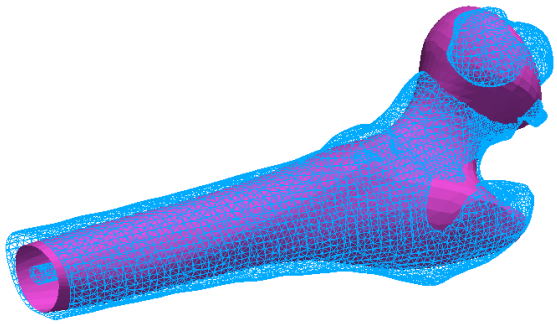

Figure 9. Transformed individualised mesh (pink colour) and mesh created with the combination of image processing algorithms (blue colour), left femur, CT series 1.

or LoG operator value is within the given threshold are considered.

Canny algorithm accepts three parameters: lower T_1 and upper T_2 threshold values and σ – the standard deviation of the Gaussian filter. Value of σ allows to control image smoothing. The bigger the σ the lesser the noise level in the image but also the bigger the blur of the image.

The LoG algorithm accepts single threshold value.

The edges detected on CT images should as much as it is possible represent the boundaries of the bone structures and omit the rest of the edges. The parameters for edge detection algorithms used in III-C were established in two ways. In case of LoG method the threshold value is automatically computed fot each input separately and it is equal to 75% of the mean value of LoG operation applied to the image. In case of Canny edge detection the global values of 3 method parameters are set for the whole image series.

To find appropriate values of parameters the set of 26 images representing different cross-sections of femur bones was selected. The images were prepared on the basis of not previously used CT data. Then the binary masks were created for the whole set, were white pixels represent the area of bone structure and black pixels represent the background. Example masks are shown in the Fig. 10.

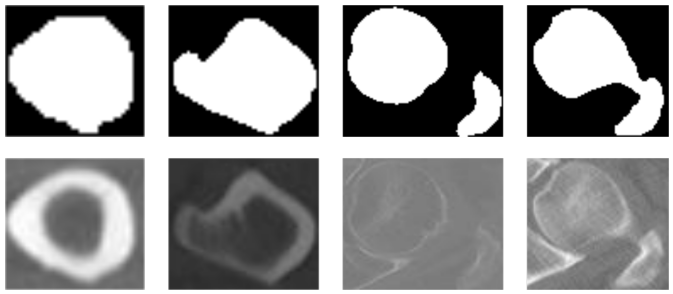

Figure 10. Sample masks images (upper row) with the corresponding CT images (bottom row).

For each of 26 mask images the set of points M, representing the boundary of the bone structure was detected with the use of method I and II of point detection described in section III-C. Then the set of points C was detected by the

Table III
RESULTS OF THE CANNY EDGE DETECTION PARAMETERS OPTIMIZATION BY PSO ALGORITHM

No.	Iterations No.	Objective function value	σ	$\mathbf{T_1}$	$\mathbf{T_2}$
1	63	2.401e04	1.4462	0.0672	0.1741
2	70	2.509e04	1.7142	0	0.1684
3	78	2.399e04	1.4463	0.0677	0.1687

same methods for images obtained with Canny edge detection filter. The parameters of the Canny edge detection filters were adjusted to minimize the distance between sets M an C described by

$$F(T_1, T_2, \sigma) = \sum_{i=1}^{L} \sum_{j=1}^{N} \|M_{ij} - C_{ij}\|, \tag{2}$$

where L is the number of images, and N is a number of rays (points) for each image.

The function F was minimized with the use of Particle Swarm Optimization algorithm (PSO). PSO algorithm is a global optimization heuristic swarm algorithm first described in [27]. The PSO algorithm was launched 3 times, in each case it ended the optimization after several dozens of iterations, when the objective function (2) did not changed its value by 40 consecutive iterations. The values of the parameters, presented in Table III were similar in all three cases. The lowest value of the objective function was achieved in the third attempt of the algorithm, thus those parameters were further used in general method.

The examples of edge detection with the use of LoG and Canny edge detection algorithms with the chosen parameters are presented in the Fig. 11.

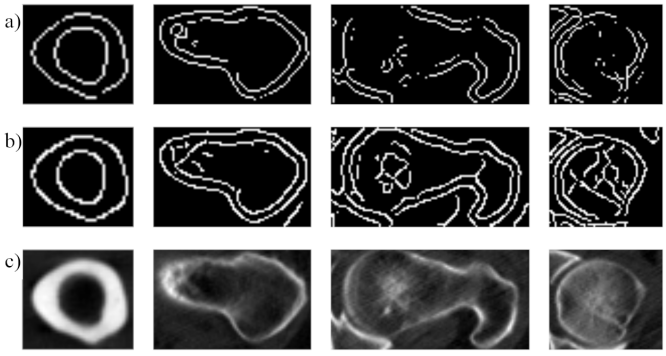

Figure 11. a) LoG edge detection b) Canny edge detection with optimized parameters c) corresponding CT images.

The number of elements of the transformed reference mesh and the number of CPD morphing algorithm iterations influence the accuracy of the transformation. In order to select the values of these parameters, their analysis was performed for left femur bone from the first data series. The algorithm was run for 3 different reference mesh densities: coarse (292 points), intermediate (1163 points) and dense (4532 points) meshes, respectively for 100, 500 and 1000 iterations of the morphing algorithm. The model was only fitted to the most challenging part of the bone — the femoral head.

The detailed results of the test are presented in Table IV, where the time measured refers to the time of CPD algorithm, similarity measure is the value of Jaccard index and dL denotes the value of change of the distance between two set of point clouds.

Table IV
THE ACCURACY OF THE LEFT FEMUR MESH FIT TO THE FIRST SERIES OF CT DATA, WITH RESPECT TO THE REFERENCE MESH DENSITY AND CPD ALGORITHM ITERATION NUMBER.

Iteration No.	Similarity measure	Measured time	dL
Mesh 1: 292 points			
100	0.708192	0 m 23.5 s	4.2072e-05
500	0.721835	1 min 59 s	1.044e-07
1000	0.722494	3 m 59 s	8.632e-10
Mesh 2: 1163 points			
100	0.754821	1 m 3 s	8.0366e-05
500	0.765219	5 m 45 s	5.062e-06
1000	0.767193	11 m 13 s	8.4806e-10
Mesh 3: 4532 points			
100	0.749425	7 m 46 s	7.1483e-05
500	0.776552	41 m 8 s	5.7644e-07
1000	0.777564	1 h 18 m 46 s	3.0411e-08

The results presented in Table II were obtained with the medium density mesh and the version of CPD algorithm which stopped after 500 iterations. Denser grid and higher number of the iterations did not significantly improve the value of similarity measure, but increased the computation time.

D. Implementation

The presented method was mainly implemented as a set of Python scripts with the use of Visualization Toolkit library with few exceptions: the YOLO network version 2 from C++ Darknet framework, created by the author of this network was used. Moreover, the detection of points on the bone structure edges and morphing algorithm were launched in MATLAB environment, due to easily available CPD implementation [29].

V. CONCLUSION

The paper presents the novel method of automatic creation of individualised bones models which incorporates the use of YOLO deep neural network, image processing algorithms and morphing procedure of the reference mesh. In order to test the method eight models of femur bones were created on the basis of four different CT datasets. The result meshes are with agreement with the expert models within the range from 77.24% to 80.83% (according to the Jaccard index). Compared to the classical methods, based purely on the image processing operations, the output model of the algorithm does not contain artefacts such as islands and holes. Due to the use of reference mesh as a base of the transformation, the structure of the resulting model does not have stairs-like

structure characteristic for voxel models. Deep neural network employed to the detection of the bone position greatly helps in automation of the method. It also achieves satisfactory results with a relatively small set (320 images) of training data.

The developed method can find application in automatic delineation of bone structures during radiotherapy planning or create a reference structure in patient positioning algorithms. Another potential application is the use of individualised models in the orthopaedic procedure planning. The model can be also easily crafted on the 3D printer and used as a visual help in bone defects recognition or to explain the idea of the orthopaedic procedure to the patient.

In the future work the authors are planning to extend the method by the use of U-net network to the task of bones segmentation and test the method accuracy for different bone structures. In case of promising results, segmentation performed by U-net network can replace currently used edge detection algorithms. It can benefit with better precision and automation of the method. To speed up the non-affine transformation step the use of fast version of CPD algorithm described in [30] can be considered. Simultaneously, the original morphing algorithm, based on [31] is being developed by the authors. The first results are encouraging and the original morphing algorithm is planned to be the default non-affine transformation method. Nevertheless, the procedure in its current shape produces potentially useful individualised bone models.

ACKNOWLEDGMENT

The authors would like to thank Maria Sklodowska-Curie National Research Institute of Oncology.

REFERENCES

[1] G. Zheng, N. P. Lutz, "Computer-Assisted Orthopedic Surgery: Current State and Future Perspective", Frontiers in Surgery, 2.12 (2015).

[2] K. Radermacher, et al., "Computer assisted orthopaedic surgery with image based individual templates", Clinical Orthopaedics and Related Research, Sep (354), pp. 28–38, (1998).

[3] J.P. Banks, "Adding Value in Additive Manufacturing: Researchers in the United Kingdom and Europe Look to 3D Printing for Customization", IEEE Pulse, 4 (2013), pp. 22–26.

[4] M. Harris, et. al. "Finite element prediction of cartilage contact stresses in normal human hips", Journal of Orthopaedic Research 30.July (2012), pp. 1133–1139.

[5] F.C. Kolo, et al. "Extreme hip motion in professional ballet dancers: Dynamic and morphological evaluation based on magnetic resonance imaging", Skeletal Radiology, 42 (2013), pp. 689–698.

[6] V. Pekar, T. R. McNutt, M.R. Kaus, "Automated model-based organ delineation for radiotherapy planning in prostatic region", International Journal of Radiation Oncology Biology, Physics 60.3 (2004), pp. 973–980.

[7] J. C. Cash, J. Fay, M. J. Dattoli, "Combined Modality Treatment for Prostate Cancer With Dynamic Adaptive Radiation Therapy Using Four-Dimensional Image-Guided Intensity-Modulated Radiation Therapy and Brachytherapy", Journal of Radiology Nursing, 28.3 (2009), pp. 87–95.

[8] S. Vasilache, et al., "Unified wavelet and gaussian filtering for segmentation of CT images; Application in segmentation of bone in pelvic CT images", BMC Medical Informatics and Decision Making, 9 (2009).

[10] T.S. Alathari, M.S. Nixon, M.T. Bah, "Femur bone segmentation using a pressure analogy", Proceedings — International Conference on Pattern Recognition (2014), pp. 972–977.

[9] J. Zhang, et al., "Fast segmentation of bone in CT images using 3D adaptive thresholding", Computers in Biology and Medicine, 40.2 (2010), pp. 231–236.

[11] F. Ding, K. Wee Kheng, T.S. Howe, "Automatic Segmentation of Femur Bones in Anterior-Posterior Pelvis X-Ray Images", Computer Analysis of Images and Patterns, 2007, pp. 205–212.

[12] J. Ehrhardt, et al., "Atlas-based segmentation of bone structures to support the virtual planning of hip operations", International Journal of Medical Informatics, vol.. 64. 2001, pp. 439–447.

[13] F. Yokota, et al., "Automated segmentation of the femur and pelvis from 3D CT data of diseased hip using hierarchical statistical shape model of joint structure". Lecture Notes in Computer Science (including subseries Lecture Notes in Artificial Intelligence and Lecture Notes in Bioinformatics), T. 5762 LNCS. 2009, pp. 811–818.

[14] H. Lamecker, et al., "A 3D statistical shape model of the pelvic bone for segmentation", Medical Imaging 2004: Image Processing, T. 5370. 2004, p. 1341.

[15] H. Seim, D. Kainmueller, M. Heller, "Automatic Segmentation of the Pelvic Bones from CT Data Based on a Statistical Shape Model", VCBM (2008), pp. 93–100.

[16] S.S. Chandra, et al., "Focused shape models for hip joint segmentation in 3D magnetic resonance images", Medical Image Analysis 18 (2014), pp. 567–578.

[17] A. Klein, et al., "Towards whole-body CT bone segmentation", Informatik aktuelll 211279 (2018), pp. 204–209

[18] F. La Rosa, "A deep learning approach to bone segmentation in CT scans", doctoral thesis, 2017. URL: http://amslaurea.unibo.it/14561/.

[19] C.M. Deniz, et al., "Segmentation of the Proximal Femur from MR Images using Deep Convolutional Neural Networks", Scientific Reports 8 (2018).

[20] S.L. Belal, "Deep learning for segmentation of 49 selected bones in CT scans: First step in automated PET/CT-based 3D quantification of skeletal metastases", European Journal of Radiology, vol. 113, pp. 89-95, 2019.

[21] J. Redmon, A. Farhadi, "YOLO9000: Better, Faster, Stronger." 2017 IEEE Conference on Computer Vision and Pattern Recognition (CVPR) (2016): 6517-6525.

[22] Z. Krawczyk, J. Starzyński, "Bones detection in the pelvic area on the basis of YOLO neural network", 19th International Conference Computational Problems of Electrical Engineering. 2018, pp. 1–4.

[23] Z. Krawczyk, J. Starzyński, "Parallel implementation of the artificial ant colony algorithm applied to medical images segmentation.", Electrical Review 1 (2017), pp. 8-11, ISSN: 0033-2097.

[24] A.V. Alvarenga, "Artificial Ant Colony: Features and applications on medical image segmentation." 2011 Pan American Health Care Exchanges (2011): 96-101.

[25] J.F. Canny, "A Computational Approach to Edge Detection." IEEE Transactions on Pattern Analysis and Machine Intelligence PAMI-8 (1986): 679-698.

[26] A. Myronenko, X. B. Song, "Point Set Registration: Coherent Point Drift." IEEE Transactions on Pattern Analysis and Machine Intelligence 32 (2010): 2262-2275.

[27] J. Kennedy, E. Russell, "Particle swarm optimization." Proceedings of ICNN'95 - International Conference on Neural Networks 4 (1995): 1942-1948 vol.4.

[28] Z. Krawczyk, J. Starzyński, "Segmentation of bone structures out of CT data: Fusion of methods," 2017 18th International Conference on Computational Problems of Electrical Engineering (CPEE), Kutna Hora, 2017, pp. 1-4.

[29] Source code: https://goope.ee.pw.edu.pl/krawczyz/bones_models.git

[30] M. Lu, J. Zhao, Y. Guo, J. Ou and J. Li, "A 3D pointcloud registration algorithm based on fast coherent point drift," 2014 IEEE Applied Imagery Pattern Recognition Workshop (AIPR), Washington, DC, 2014, pp. 1-6.

[31] J. Starzyński, M. Borysiak, Z. Krawczyk, "Creating patient-specific Finite Element Models with a Simple Mesh Morpher", Computer Applications in Electrical Engineering, 8/2010 pp: 38-45, ISSN: 1508-4248.